Title: Reorganization and reactivation of a preexisting taste-responsive hippocampal network

Authors: Linnea E. Herzog[1], Donald B. Katz[1,2,3], and Shantanu P. Jadhav[1,2,3,*]

Affiliations:

[1]Graduate Program in Neuroscience, Brandeis University, Waltham, MA, 02453, USA

[2]Neuroscience Program, Department of Psychology, and Volen National Center for Complex Systems, Brandeis University, Waltham, MA, 02453, USA

[3]Lead Contact

*Correspondence to: shantanu@brandeis.edu (S.P.J.)

Summary

Animals need to remember the locations of nourishing and toxic food sources for survival, a fact that necessitates a mechanism for associating taste experiences with particular places. We have previously identified such responses within hippocampal place cells [1], the activity of which is thought to aid memory-guided behavior by forming a mental map of an animal's environment that can be reshaped through experience [2-7]. It remains unknown, however, whether specific place cells are preconfigured to respond to tastes, or whether taste-responsiveness emerges as a result of experience that reorganizes spatial maps. Here, we recorded from neurons in the dorsal CA1 hippocampal region of rats running for taste rewards delivered *via* intra-oral cannulae at specific locations on a linear track. We found that taste responsiveness was inherent to a subset of cells that, even prior to taste delivery, had larger place fields than non-taste-responsive cells overlapping with stimulus delivery zones. Taste-responsive cells' place fields then contracted, as a result of taste exposure, to be more restricted to stimulus delivery zones, leading to a stronger representation of rewarded areas on the track. These remapped units exhibited increased sharp-wave ripple co-activation during the taste delivery session, which correlated with the degree of place field contraction. Our results suggest that taste responsivity is preconfigured in a subset of hippocampal place cells, whose spatial representations are then refined by sensory experience to signal reward. This represents a possible mechanism by which animals identify and remember locations where ecologically relevant stimuli are found within their environment.

Keywords

Hippocampus, Taste, Chemosensation, Place cells, Remapping, Sharp-wave ripple, Co-activation, Reactivation

Results and Discussion

To investigate how place cells responded to tastes during running, we recorded the activity of CA1 neurons (*n* = 212, mean ± SEM: 23.6 ± 4.12 neurons/session; **Figure S1A**) as rats performed a linear track alternation task (**Figure 1A**). Each experimental day consisted of three track-running sessions ('Pre,' 'Tastes,' and 'Post') interleaved with rest sessions in a sleep box. During the 'Pre' and 'Post' probe sessions, rats explored the track in the absence of tastes. During the 'Tastes' session, rats received aliquots of either sweet or salty tastes, delivered directly to the tongue *via* intra-oral cannula when the rats reached either of two designated locations along the track. Isolated units were classified as putative pyramidal cells (83.5%, 177/212) or interneurons (16.5%, 35/212) based on spike width and firing rate (**Figure S1B**). Most pyramidal cells (97.2%, 172/177) could be categorized as place cells (see STAR Methods, [1, 8]), a subset of which (*n* = 44/172) responded to tastes (**Figure 1B**, **Table S1**). Taste responses were observed only in cells with place fields overlapping taste delivery zones (**Figure 1C**), supporting previous work demonstrating that hippocampal sensory responses are gated by place cells' spatial firing properties [1, 8, 9].

We previously established that taste-responsive cells tend to exhibit less spatial selectivity than non-taste-responsive cells [1]. However, it remains unclear whether or how these spatial properties develop as a consequence of taste experience. We therefore compared the place field sizes of taste-responsive (*n* = 38) and non-taste-responsive (*n* = 79) cells before and after the animals' first exposure to the zoned tastes paradigm (**Figure 2A**). Taste-responsive cells proved to have larger place fields than non-taste-responsive cells even before the rats' first exposures to saccharin and NaCl solutions (**Figure 2B**), such that taste-responsiveness could be predicted in taste-naïve subjects. This relationship between place field size and taste responsiveness (**Figure S2**) demonstrates that gustatory receptivity is to some degree "built-into" the system—that a non-random subset of neurons is pre-wired to respond to taste stimuli, perhaps reflecting differential input from the medial (MEC) and lateral (LEC)

entorhinal cortices, which represent the two major cortical inputs to the hippocampus, encoding spatial and non-spatial information, respectively [10-13].

Following the Tastes session, meanwhile, taste-responsive cells' place fields shrink, becoming comparable to those of non-taste-responsive place cells (**Figure 2B**); that is, taste-responsive cells became more spatially selective with taste experience. Since place fields are known to accumulate in rewarded locations [14, 15], it is reasonable to hypothesize that this remapping might function to localize place fields to taste delivery zones. However, we observed relatively few instances of location remapping in taste-responsive (n = 44) and non-taste-responsive (n = 128) cells (**Figure 3A**) — no overall differences in Pre-Post place field location or place field-taste zone distance were found between groups (**Figure 3B**). Instead, taste-responsive cells exhibited high spatial overlap with taste delivery zones from the Pre session. Contraction of their place fields with taste experience decreased overall overlap (**Figure 3C**), but increased place field density in the delivery zones, such that the place field peaks of taste-responsive units tended to more reliably overlap with taste zones in the Post session (**Figure 3D**), and these cells' overall spatial coverage came to form a bimodal distribution whose peaks roughly coincided with locations of taste delivery (**Figure 3E**).

In summary: taste-responsive cells initially have large place fields that overlap with future locations of taste delivery; these place fields then contract with taste experience, leading to a more precise representation of taste delivery locations in animals' mental maps of the track. Non-taste-responsive cells do not exhibit this effect, instead tiling the track continuously during taste experience.

One possible mechanism underlying this representational reorganization is the co-firing of goal-related assembly patterns during sharp-wave ripples (SWRs; [16, 17]), a high-frequency hippocampal oscillation that is necessary for memory consolidation during wake [18] and sleep [19]. During ripples, the activity of sequences of place cells is typically "replayed" in a time-compressed manner [20, 21]; sensory cues are known to influence this SWR reactivation [22]

and replay content [23]. We therefore hypothesized that taste-responsive place cells would exhibit particularly strong SWR co-activation during waking behavior and sleep, as reorganization occurred.

To test this hypothesis, we identified SWR co-activation events (**Figure S3A**) in taste- and non-taste-responsive cell pairs (**Figure S3B**) whose place fields exhibited high and low spatial overlap. As expected [20, 24-26], highly overlapping cell pairs co-fired more during wake and sleep SWRs than pairs with low overlap (**Figure 4A**). This effect persisted when we calculated the mean co-activation differences for all possible combinations of cell pairs (Taste/Taste or Non/Non – Taste/Non) across sleep and wake (**Figure 4B**). Highly overlapping taste-responsive cell pairs exhibited higher co-activation differences than similarly overlapping non-taste-responsive cell pairs during the taste experience session and during both pre- and post-experience sleep (**Figure 4B**). This effect parallels the changes observed in place field size and spatial coverage on the track—we saw that taste-responsive cells' place fields contract over areas of taste delivery during the Tastes session, while non-taste-responsive cells remain stable across taste experience. Furthermore, we observed a significant correlation between place field contraction (from Pre to Post) and SWR reactivation probability during the Tastes session (**Figure 4C**). These data support the hypothesis that reactivation during SWRs could play an important role in stabilizing animals' mental maps as they encounter tastes within their environment, with taste-responsive units coming to more precisely signify areas where food can be found.

Overall, our data show that taste responsivity is preconfigured in a subset of hippocampal place cells, which exhibit differences in spatial selectivity prior to taste experience on the track, compared to non-taste-responsive cells. The experience of receiving tastes in particular locations leads to the contraction of taste-responsive cells' place fields over taste delivery zones—a reorganization of animals' internal representations of the track to emphasize locations of taste consumption. The idea that rewarding or aversive experiences can reorganize

hippocampal representations of an environment to encode points of behavioral salience is not new [14, 15, 27, 28], but we have shown that these shifts arise from changes in the spatial properties of a preconfigured group of sensory-responding cells. One possible mechanism underlying this shift is the increased SWR co-activation of taste-responsive units with high spatial overlap, which correlated with the degree of place field contraction that we observed during taste experience. Our findings are consistent with previous observations that introducing salient stimuli, whether rewarding [14, 15] or aversive [27, 28], leads to the increased reactivation of behaviorally relevant trajectories during SWRs and reorganizes animals' hippocampal representations to map out areas of high salience within an environment. These results provide further evidence for a flexible memory framework where hippocampal neurons can multiplex contextual information and sensory cues to update animals' mental maps of an environment [4, 29-32].

Acknowledgments

This work was supported by the Alfred P. Sloan Foundation (Sloan Research Fellowship in Neuroscience to S.P.J.), the Whitehall Foundation (S.P.J.), and the National Institutes in Health (NIH Grants R01 DC006666 and R01 DC007703 to D.B.K. and Training Grant T90 DA032435 to L.E.H.).

Author Contributions

All authors contributed to all aspects of this report.

Declaration of Interests

The authors declare no competing interests.

Figure Legends

Figure 1. Experimental design and example taste responses.

A, Schematic of an example zoned taste experiment. Each experiment day consisted of seven sessions: three track-running sessions (Pre, Tastes and Post), interleaved with four sleep sessions (S1-4). For the Pre and Post probe sessions, rats ran on the track in the absence of tastes. During the Tastes session, rats received a randomized delivery of either sweet (green = S, 4 mM saccharin) or salty (yellow = N, 100 mM sodium chloride) taste solution upon entering either of the two designated regions on the track (Zone 1 and Zone 2). Neurons from the dorsal CA1 hippocampal region were recorded continuously throughout all track-running and sleep sessions (see also **Figure S1** and **Table S1**). ***B***, Example in- and out-of-field responses for a taste-responsive and non-taste-responsive place cell. The 1D linearized and line plots are shown for each cell during the Pre, Tastes and Post sessions. The firing map for the Tastes session was computed with taste delivery periods (500 ms before to 2500 after taste delivery) omitted from the analysis. Numbers on each plot denote peak spatial firing rate (FR) in Hz. Taste delivery locations are denoted by the colored symbols (green: S, 4 mM saccharin; yellow: N, 100 mM sodium chloride), with the in-field trials outlined in pink. Middle panels depict raster plots of each cell's in- and out-of-field responses to each taste. Black dots indicate spike times during each individual trial aligned to the time of taste delivery. Bottom panels show the evoked responses to taste deliveries taking place in- and out-of-field for each cell. Each colored trace represents the mean firing rate to saccharin or NaCl. Note that taste responses are only found within the taste-responsive cell's place field. ***C***, Magnitude of taste responsiveness and specificity (η^2) for the in- and out-of-field regions of taste- (n = 23) and non-taste-responsive (n = 25) cells that met our criteria ($\geq$ 10 trials in- and out-of-field). The mean η^2 for the in-field region of taste-responsive cells was higher (2-way ANOVA, cell type: **p = 0.0048, epoch: ***p = 0.0005, interaction: p = 0.15) than that of non-taste-responsive cells (*p = 0.018), as well as the out-of-field region of either taste- (**p = 0.0043) or non-taste-responsive cells (***p = 8.1e-05),

indicating that taste responses were observed only in cells with place fields overlapping taste delivery zones.

Figure 2. Taste-responsive place cells become spatially selective after taste experience. ***A***, Example spatial firing maps and line plots of four taste- and non-taste-responsive place cells during the Pre and Post sessions. Numbers on each plot denote peak spatial firing rate (FR) in Hz. Place field boundaries during each session are indicated by pink shading. Note that the taste-responsive cells' place fields start out large, then decrease in size after taste experience. ***B***, Left, linearized firing field size for taste- (n = 38) and non-taste-responsive (n = 79) place cells on the first experiment day, normalized as a fraction of track coverage. The mean place field size of taste-responsive cells prior to taste experience is larger (2-way ANOVA, cell type: ***p = 9.8e-06, epoch: **p = 0.0037, interaction: p = 0.052) than that of non-taste-responsive cells (***p = 2.8e-05), as well as both taste- (*p = 0.016) and non-taste-responsive cells (***p = 8.1e-07) after taste experience (see also **Figure S2**).

Figure 3. Taste-responsive cells' place fields contract around areas of taste delivery. ***A***, Spatial firing maps of four example taste- and non-taste-responsive cells during the Pre and Post track-running sessions. Numbers on each plot denote peak spatial firing rate (FR) in Hz. Place field (PF) boundaries during each session are indicated by pink shading, while the peak distributions of trials during the Tastes session (taste zone, or TZ) are indicated by gray boxes. Note how the taste-responsive cells' place fields overlap with the locations of taste delivery across taste experience, while the majority of non-taste-responsive cells' do not. ***B***, Change in PF peak location and PF-TZ distance from Pre to Post. No differences in the mean Δ PF peak location (unpaired t-test, p = 0.97) or Δ PF-TZ distance (unpaired t-test, p = 0.58) were observed between groups or shuffled controls (paired t-tests, Δ PF peak location: Taste vs. Shuffle: p = 0.45, Non vs. Shuffle: p = 0.15; Δ PF-TZ distance, Taste vs. Shuffle: p = 0.84, Non

vs. Shuffle: p = 0.65), indicating that taste- and non-taste-responsive cells exhibited comparable remapping of peak location from the Pre to Post session. ***C***, Mean PF-TZ overlap for taste- and non-taste-responsive cells before and after taste experience. The place fields of taste-responsive cells had a greater overlap with taste delivery zones prior to taste experience (2-way ANOVA, cell type: ***p = 6.2e-11, epoch: p = 4.5e-08, interaction: **p = 0.0024) than non-taste-responsive cells (***p = 1.2e-10), as well as taste- (***p = 5e-06) or non-taste-responsive cells (***p = 6.7e-16) after taste experience. ***D***, Proportion of taste- and non-taste-responsive cells with peak place field firing in TZ. Bars show the percentage of cells with place field peaks located within the taste zone, compared to chance level (calculated based on average TZ coverage of the track). A greater-than-chance proportion of taste-responsive cells had place field peaks in the TZ during Post (binomial test, ***p = 3.7e-05), underscoring that the decrease of overlap for taste-responsive cells in ***C*** is due to the contraction of place fields around taste delivery zones. ***E***, Distribution of place field coverage before and after taste experience for taste- and non-taste-responsive units. The session-averaged TZ are indicated by gray boxes. Histograms indicate the number of cells present at each spatial location on the track. Note how the place fields of taste-responsive cells initially span the track during Pre (Hartigan's dip test for bimodality, dip = 0.058, p = 0.31), then contract over TZ during Post to form a bimodal distribution (dip = 0.081, *p = 0.018), while non-taste-responsive place fields tile the track during Pre (dip = 0.033, p = 0.40) and Post (dip = 0.040, p = 0.15).

Figure 4. Remapped units exhibit increased SWR co-activation during taste experience. ***A***, Spatial firing plots and awake and sleep SWR co-activation for three example cell pairs (taste-responsive pairs with high and low overlap, non-taste-responsive pair with high overlap) during track running sessions (see also **Figure S3**). Numbers on each place map plot denote peak spatial firing rate (FR) in Hz. Place field (PF) boundaries during each session are indicated by pink lines. The bar plots show the Z-scored co-activation for each cell pair during wake and

sleep SWRs. Note how the high overlap pairs exhibit more co-activation than the low overlap pairs. ***B***, SWR co-activation differences between taste- and non-taste-responsive cell pairs across taste experience. Bars display the mean difference in SWR co-activation between same (Taste/Taste or Non/Non) and different (Taste/Non) taste pairs for all significant co-activation events. Significant differences were found for both wake (3-way ANOVA, cell type: ***p = 3.3e-04, overlap: ***p = 0, cell type x epoch: **p = 0.0061, cell type x overlap: ***p = 0) and sleep (cell type: ***p = 4.5e-15, epoch: *p = 0.024, overlap: ***p = 3e-28, cell type x overlap: ***p = 4.1e-04, epoch x overlap: **p = 0.0037, cell type x epoch x overlap: ***p = 6.4e-04). Post hoc comparisons revealed that taste-responsive cell pairs with high overlap had higher mean co-activation differences than non-taste-responsive cell pairs during taste experience (*p = 0.044), and both pre- (*p = 0.022) and post-experience (***p = 6e-08) sleep. ***C,*** Each cells' reactivation probability during the Tastes session (x-axis) is plotted against the decrease in PF size from the Pre to Post session (y-axis). The significant correlation (Pearson's correlation, n = 172 place cells, r = 0.20, **p = 0.0081) suggests that the observed increase in reactivation plays a role in reorganizing animal's mental maps to better represent locations of taste delivery after experience.

STAR Methods

Contact for Reagent and Resource Sharing

Further information and requests for resources should be directed to the Lead Contact, Dr. Shantanu P. Jadhav (shantanu{at}brandeis.edu).

Experimental Model and Subject Details

Five adult male Long-Evans rats (450-550 g, 4-6 months) served as subjects in this study. Rats were individually housed and kept on a 12 h light/dark cycle, with all sessions taking place around the same time during the light period. All surgical and experimental procedures were conducted in accordance with the National Institutes of Health guidelines and approved by the Brandeis University Institutional Animal Care and Use Committee.

Method Details

Experimental design

After several weeks of habituation to daily handling, animals were pre-trained to seek water on an elevated linear track as described previously [18] and habituated to an elevated, opaque sleep box. After animals learned to alternate on the linear track, they were chronically implanted with a multi-tetrode drive and an intra-oral cannula (see *Surgical implantation and electrophysiology*).

Following recovery from the implantation surgery (~7-8 days), rats were water-deprived to 85-90% of their *ad libitum* weight and re-trained on the linear track, during which time they were also habituated to the sleep box and the delivery of water through the intra-oral cannula. At ~14 d after implantation, we performed daily recording sessions in which rats ran on the linear track for taste stimuli delivered in two locations (see **Figure 1A** and *Zoned taste paradigm*). Following the conclusion of these zoned taste experiments, additional recordings were conducted while rats received a battery of basic tastes; data from these experiments has been presented previously to demonstrate that hippocampal neurons respond to tastes [1].

Following the conclusion of all experiments, we made electrolytic lesions through each electrode tip to mark recording locations. After 12-24 hours, animals were euthanized and intracardially perfused with 4% formaldehyde using approved procedures. Brains were fixed for 24-48 hours, cryoprotected (30% sucrose in 4% formaldehyde), and stored at 4°C. Brains were sectioned into 50 µm slices and stained with cresyl violet to confirm electrode placement in the hippocampal cell layer (**Figure S1A**).

Zoned taste paradigm

Each recording session typically lasted between 2 and 3 hours, and consisted of three running sessions on a 150 cm elevated linear track interleaved with four 15-20 minute sleep sessions in a ~30 x 30 x 40 cm black box (rest box). The first (Pre) and last (Post) sessions on the linear track consisted of 15-20 minute periods in which animals were habituated to the track in the absence of tastes. During the 30-90 minute Tastes session, rats received a pseudo-randomized delivery of either a sweet [4 mM saccharin (S)] or salty [100 mM sodium chloride (N)] taste solution at designated areas ("taste zones," or TZ) located approximately 1/3 and 2/3 of the way down the track. The rat's position was detected in real-time with an overhead monochrome CCD camera (30 fps) and LEDs affixed to the recording headstage, and used to trigger taste deliveries when animals entered into one of the two taste delivery zones. Taste solutions were delivered directly onto the tongue in ~40 µL aliquots via two polyamide tubes inserted into the intra-oral cannula, with a separate tube for each solution to prevent the mixing of tastes. Animals had access to an additional 15-20 mL of water in their home cage after the end of each experiment day.

Surgical implantation and electrophysiology

Following pre-training on the linear track and habituation to the sleep box, animals were implanted with a microdrive array consisting of 25-30 independently moveable tetrodes in the right dorsal hippocampal region CA1 (-3.6 mm AP, 2.2 mm ML), and an intra-oral cannula. Each intra-oral cannula consisted of a polyethylene tube inserted beneath the left temporalis muscle

and terminating anterolateral to the first maxillary molar, allowing for the precise delivery of taste solutions onto the rat's tongue [33-35].

Electrophysiological recordings were conducted using a SpikeGadgets system [36]. Spikes were sampled at 30 kHz and bandpass filtered between 600 Hz and 6 kHz. Local field potentials (LFPs) were sampled at 1.5 kHz and bandpass filtered between 0.5 and 400 Hz. Over ~14 d following surgery, tetrodes were gradually advanced to the CA1 hippocampal cell layer, as identified by characteristic EEG patterns (SWRs; theta rhythm) as previously described [18, 36, 37]. Tetrodes were readjusted after each day's recordings. Each animal had one hippocampal reference tetrode in corpus callosum, which was also referenced to a ground screw installed in the skull overlying cerebellum.

Unit inclusion

Spikes were sorted as described previously [1, 36, 37]. In brief, single units were isolated offline based on peak amplitude and principal components (Matclust, M.P. Karlsson). Only well-isolated units with stable waveforms that fired at least 100 spikes per session were included in our analysis. Putative interneurons (*Int*) were identified on the basis of firing rate (> 8.5 Hz) and spike width (< 0.35 ms) parameters (**Figure S1B**). All other isolated units were classified as putative pyramidal cells (*Pyr*). We isolated a total of 212 neurons from five rats, conducted across nine experiments. **Table S1** shows the distribution of cells across all five animals.

<u>Quantification and Statistical Analysis</u>

Sharp-wave ripple detection

SWRs were detected as previously described [36, 37] using the ripple-band (150-250 Hz) filtering of LFPs from multiple tetrodes. A Hilbert transform was used to determine the envelope of band-passed LFPs, and events that exceeded a threshold (mean + 3 SD) were detected. SWR events were defined as the times around initially detected events when the envelope exceeded the mean. SWR periods were excluded from place field analysis, similar to previous studies [1, 36, 37].

Taste response properties

Hippocampal responses to tastes were characterized as described previously ([1]; for characterization of response properties in other parts of the taste system, see [35, 38-41]. Since we have already extensively described the coding content of taste responsiveness in these neurons [1], and given our use of only two tastes in the current context, here we perform (except when noted, see *Taste selectivity* below) a simpler test of taste responsiveness. In brief, neurons were classified as taste-responsive if they exhibited responses to taste presence (divergence from baseline) and/or identity (taste-specific differences in evoked firing) in the 2500 ms of spiking activity following each taste delivery; all other units were classified as non-taste-responsive (see **Figure 1B** for examples).

Taste selectivity

The magnitude of taste responsiveness and specificity for each cell was quantified using eta-squared (η^2), a standard measure of ANOVA effect sizes that describes the proportion of variance in a dependent variable explained by each factor:

$$\eta^2 = SS_{(factor)}/SS_{(total)},$$

where SS is the sum of squares [1, 42]. In our analysis, we used the summed SS of the two main factors (time + taste) to calculate η^2. As described below (see *In-field vs. out-of-field analysis*), a 2-way ANOVA was used to assess differences in η^2 for the in-field and out-of-field regions of taste-responsive (n = 23) and non-taste-responsive (n = 25) place cells that fit our analysis criteria (> 1 Hz place field peak, $\geq$ 10 in- and out-of-field trials; **Figure 1C**).

Spatial maps

To visualize the spatial firing properties of neurons, 2D position data were converted to linear positions, and one-dimensional occupancy-normalized firing rate maps (**Figure 1B**, **2A**, **3A**, **4B**) were constructed using 2 cm bins and smoothed with a 1D Gaussian (σ = 5 cm) as previously described [18, 36]. Data from taste delivery (500 ms before to 2500 ms after taste delivery),

SWR periods (see *Sharp-wave ripple detection*), and periods of immobility (< 3 cm/s) were excluded from spatial map analysis.

Peak rates for each cell were defined as the maximum firing rate across all spatial bins in the spatial map. Each cell's place field was defined as the largest cluster of neighboring spatial bins which had firing rates $\geq$ 20% of the peak rate; place field sizes were then calculated by multiplying the number of bins by the bin size [43]. To compare place field sizes across sessions, place field size was normalized as a fraction of the track. A 2-way ANOVA was used to determine whether the mean place field size differed significantly between taste-responsive (n = 38) and non-taste-responsive (n = 79) place cells before and after the first session of zoned taste experience (**Figure 2B**). The percentages of taste- and non-taste-responsive cells in each spatial bin (0.2*n as a fraction of track coverage) were compared using χ^2 tests (**Figure S2A**). A plot of the percentage of taste-responsive cells in each spatial bin was also constructed (**Figure S2B**).

To determine how taste experience affects place field position (**Figure 3B**), the mean change in place field peak location (Δ PF peak location) and place field-taste zone distance (Δ PF-TZ distance) from Pre to Post were compared for taste- (n = 44) and non-taste-responsive (n = 128) cells using unpaired t-tests. The taste zones were defined separately for each experiment day using a Gaussian fit to determine the peak distribution of trial locations during the Tastes session (defined as $\mu \pm \sigma$ for the normal distribution of all trial locations, calculated separately for each delivery zone).The closest taste zone to a place field's peak location was used to calculate PF-TZ distance. Paired t-tests were used to compare both the mean Δ PF peak location and Δ PF-TZ distance for each group with controls that were calculated by randomly shuffling values from the Post session.

To compare the PF-TZ overlap across sessions (**Figure 3C**), the track was divided into 100 spatial bins, and we calculated which bins each PF and TZ spanned along the normalized track. PF-TZ overlap was defined as the number of taste zone locations that overlapped with a

cell's place field, divided by the total number of taste zone locations. 2-way ANOVAs were used to compare the PF-TZ overlap between taste- and non-taste-responsive cells before and after taste experience.

To determine if greater-than-chance numbers of cells in any group had place field peaks inside the taste delivery zone (**Figure 3D**), binomial tests were used to compare the observed vs. expected proportions of taste-responsive and non-taste-responsive cells with PF peaks in the TZ during Pre and Post. The expected proportion (32%) was calculated based on the average TZ coverage of the track, operating under the assumption that place fields exhibit equal coverage of the track.

To compare place field coverage before and after taste experience (**Figure 3E**), locations with place field coverage were combined to create a histogram of all place field locations (bin size = 6 cm) for taste- and non-taste-responsive units before and after experience. Hartigan's dip test for bimodality was used to compare the spatial coverage of taste- and non-taste-responsive cells during Pre and Post (n = 44 taste-responsive cells, n = 128 non-taste-responsive cells, n = 1000 bootstrap iterations).

In-field vs. out-of-field analysis

To analyze how place cells responded to tastes delivered inside or outside of their place fields (**Figure 1B**), only pyramidal cells exhibiting place-specific activity (n = 172 cells, defined as neurons whose peak rate exceeded 1 Hz) were considered. Only place cells that contained at least ten in- and out-of-field deliveries of each taste were included in this analysis (n = 23 taste-responsive cells, n = 25 non-taste-responsive cells). A 2-way ANOVA was used to assess differences between the mean in-field and out-of-field taste response magnitude (calculated using η^2, see *Taste selectivity*) of taste-responsive and non-taste-responsive cells (**Figure 1C**).

SWR co-firing

SWRs co-activation events were defined as ripples during which both cells in a given cell pair fired spikes (example in **Figure S3A**; locations of all awake ripples and co-firing events are

plotted in **Figure S3B**). Co-activation of cell pairs during awake and sleep SWRs was calculated as previously described [26], using a Z-score to compare cells with different activity levels (see right panels of **Figure 4A**). Only cell pairs that fired at least 100 spikes per session, had a peak firing rate exceeding 3 Hz during run sessions, and co-fired at least 5 times during SWRs were considered for analysis. Place field overlap for pairs of cells was defined as twice the sum of the overlapping areas of the linear rate curves divided by the sum of the areas of each curve [18]; all cell pairs with overlap $\geq$ 0.5 were classified as high overlap (see examples in top and bottom panels of **Figure 4A**), while all cell pairs with overlap < 0.5 were classified as low overlap (see example in middle panel of **Figure 4A**). For sleep SWRs, the closest running session was used to calculate spatial overlap.

The mean co-activation difference was defined as the difference in Z-scored co-activation between all combinations of same (Taste/Taste or Non/Non) – different (Taste/Non) cell pairs during awake running sessions (Pre, Tastes and Post) as well as the Pre rest session before the run sessions and the Post rest sessions after taste experience (averaged across the two rest sessions, S3 and S4). For these comparisons, same cell pairs (Taste or Non) with a greater spatial overlap than their corresponding different cell pair were classified as high overlap (High), while same cell pairs with a smaller spatial overlap than their corresponding different cell pair were classified as low overlap (Low). A 3-way ANOVA was used to compare the cell type, overlap and epoch effects on the mean co-activation difference during awake and sleep SWRs (**Figure 4B**; number of same-different cell pair combinations; wake: n = 96 Pre/Taste/High, n = 325 Pre/Non/High, n = 96 Pre/Taste/Low, n = 308 Pre/Non/Low, n = 74 Tastes/Taste/High, n = 320 Tastes/Non/High, n = 118 Tastes/Taste/Low, n = 313 Tastes/Non/Low, n = 107 Post/Taste/High, n = 311 Post/Non/High, n = 85 Post/Taste/Low, n = 322 Post/Non/Low; sleep: n = 213 Pre/Taste/High, n = 638 Pre/Non/High, n = 141 Pre/Taste/Low, n = 870 Pre/Non/Low, n = 512 Post/Taste/High, n = 5402 Post/Non/High, n = 371 Post/Taste/Low, n = 4072 Post/Non/Low).

In order to assess the relationship between SWR activation and remapping (**Figure 4C**), the reactivation probability was computed for all units as previously described [15]; a Pearson's correlation between reactivation probability and the difference in PF size from the Pre to Post sessions was then calculated.

Statistical analysis

All statistical tests were performed using custom routines in MATLAB (MathWorks, Natick, MA, RRID: SCR_001622) and evaluated at a level of $\alpha = 0.05$, with a Bonferroni correction applied for multiple comparisons. Unless otherwise noted, values and error bars in the text denote means ± SEM.

Data and Software Availability

The data and code used in this study are available upon reasonable request by contacting the Lead Contact, Dr. Shantanu P. Jadhav (shantanu{at}brandeis.edu).

Supplemental Information titles and legends

Figure S1. Histology and unit classification, related to Figure 1.

A, Histological verification of tetrode locations in intermediate dorsal CA1. ***B***, Classification of putative interneurons (Int, gray crosses) from pyramidal cells (Pyr, black circles) based on spike width (> 8.5 Hz) and firing rate (< 0.35 ms) parameters.

Table S1. Cell distribution across animals, related to Figure 1.

Summary of the number of taste-responsive and total CA1 cells recorded from each animal. Only cells meeting the inclusion criteria (see STAR Methods) are reported. Putative pyramidal cells (Pyr) and interneurons (Int) were identified on the basis of firing rate and spike width parameters. Neurons were classified as “taste-responsive” if they exhibited responses to taste presence or identity.

Figure S2. Taste responsiveness is related to place field size during the Pre session, related to Figure 2.

A, Histogram of taste-responsive and non-taste-responsive place field sizes. Stacked bars represent the percentage of cells within each cell type that fell within a given size bin (n*0.2 as a fraction of the track). Cells with smaller place fields were more likely to be non-taste-responsive (PF size < 0.2, χ^2 test, χ = 12.2, ***p = 4.9e-04), while cells with larger place fields were more likely to be taste-responsive (PF size = 0.4-0.6, χ = 10.9, ***p = 9.7e-04; PF size > 0.6, χ = 8.9, **p = 0.0029). ***B***, Likelihood of taste-responsiveness as a function of PF size. Each bar represents the percentage of taste-responsive (TR) cells in each size bin, which increases with increasing place field size.

Figure S3. SWR co-activation and distribution of significant events along the track, related to Figure 4.

A, Example of one co-activation event following a taste trial, with saccharin delivery denoted by the vertical green line. Spikes from two taste-responsive cells are shown in black, with spikes that occurred during the same SWR inside the purple bar. SWRs were detected using the simultaneously recorded EEG filtered at 150-250 Hz (black traces above raster plot). The top trace shows the SWR in higher magnification. ***B***, Probability of SWRs and significant co-activation events for taste- and non-taste-responsive cell pairs at each location on the track during awake running sessions.

References

1. Herzog, L.E., Pascual, L.M., Scott, S.J., Mathieson, E.R., Katz, D.B., and Jadhav, S.P. (2019). Interaction of taste and place coding in the hippocampus. J Neurosci *39*, 3057-3069.
2. Muller, R. (1996). A quarter of a century of place cells. Neuron *17*, 813-822.
3. Martin, S.J., and Clark, R.E. (2007). The rodent hippocampus and spatial memory: from synapses to systems. Cell Mol Life Sci *64*, 401-431.
4. Colgin, L.L., Moser, E.I., and Moser, M.B. (2008). Understanding memory through hippocampal remapping. Trends Neurosci *31*, 469-477.
5. Eichenbaum, H. (2017). The role of the hippocampus in navigation is memory. J Neurophysiol *117*, 1785-1796.
6. Schiller, D., Eichenbaum, H., Buffalo, E.A., Davachi, L., Foster, D.J., Leutgeb, S., and Ranganath, C. (2015). Memory and space: towards an understanding of the cognitive map. J Neurosci *35*, 13904-13911.
7. Ekstrom, A.D., and Ranganath, C. (2018). Space, time, and episodic memory: the hippocampus is all over the cognitive map. Hippocampus *28*, 680-687.
8. Moita, M.A., Rosis, S., Zhou, Y., LeDoux, J.E., and Blair, H.T. (2003). Hippocampal place cells acquire location-specific responses to the conditioned stimulus during auditory fear conditioning. Neuron *37*, 485-497.
9. Shan, K.Q., Lubenov, E.V., Papadopoulou, M., and Siapas, A.G. (2016). Spatial tuning and brain state account for dorsal hippocampal CA1 activity in a non-spatial learning task. eLife *5*.
10. Li, Y., Xu, J., Liu, Y., Zhu, J., Liu, N., Zeng, W., Huang, N., Rasch, M.J., Jiang, H., Gu, X., et al. (2017). A distinct entorhinal cortex to hippocampal CA1 direct circuit for olfactory associative learning. Nat Neurosci *20*, 559-570.

11. Van Cauter, T., Camon, J., Alvernhe, A., Elduayen, C., Sargolini, F., and Save, E. (2013). Distinct roles of medial and lateral entorhinal cortex in spatial cognition. Cereb Cortex *23*, 451-459.

12. Wang, C., Chen, X., Lee, H., Deshmukh, S.S., Yoganarasimha, D., Savelli, F., and Knierim, J.J. (2018). Egocentric coding of external items in the lateral entorhinal cortex. Science *362*, 945-949.

13. Hargreaves, E.L., Rao, G., Lee, I., and Knierim, J.J. (2005). Major dissociation between medial and lateral entorhinal input to dorsal hippocampus. Science *308*, 1792-1794.

14. Hollup, S.A., Molden, S., Donnett, J.G., Moser, M.B., and Moser, E.I. (2001). Accumulation of hippocampal place fields at the goal location in an annular watermaze task. J Neurosci *21*, 1635-1644.

15. Singer, A.C., and Frank, L.M. (2009). Rewarded outcomes enhance reactivation of experience in the hippocampus. Neuron *64*, 910-921.

16. Dupret, D., O'Neill, J., Pleydell-Bouverie, B., and Csicsvari, J. (2010). The reorganization and reactivation of hippocampal maps predict spatial memory performance. Nat Neurosci *13*, 995-1002.

17. Girardeau, G., and Zugaro, M. (2011). Hippocampal ripples and memory consolidation. Curr Opin Neurobiol *21*, 452-459.

18. Jadhav, S.P., Kemere, C., German, P.W., and Frank, L.M. (2012). Awake hippocampal sharp-wave ripples support spatial memory. Science *336*, 1454-1458.

19. Girardeau, G., Benchenane, K., Wiener, S.I., Buzsaki, G., and Zugaro, M.B. (2009). Selective suppression of hippocampal ripples impairs spatial memory. Nat Neurosci *12*, 1222-1223.

20. Lee, A.K., and Wilson, M.A. (2002). Memory of sequential experience in the hippocampus during slow wave sleep. Neuron *36*, 1183-1194.

21. Carr, M.F., Jadhav, S.P., and Frank, L.M. (2011). Hippocampal replay in the awake state: a potential substrate for memory consolidation and retrieval. Nat Neurosci *14*, 147-153.

22. Eschenko, O., Ramadan, W., Molle, M., Born, J., and Sara, S.J. (2008). Sustained increase in hippocampal sharp-wave ripple activity during slow-wave sleep after learning. Learn Mem *15*, 222-228.

23. Ji, D., and Wilson, M.A. (2007). Coordinated memory replay in the visual cortex and hippocampus during sleep. Nat Neurosci *10*, 100-107.

24. Wilson, M.A., and McNaughton, B.L. (1994). Reactivation of hippocampal ensemble memories during sleep. Science *265*, 676-679.

25. Foster, D.J., and Wilson, M.A. (2006). Reverse replay of behavioural sequences in hippocampal place cells during the awake state. Nature *440*, 680-683.

26. Cheng, S., and Frank, L.M. (2008). New experiences enhance coordinated neural activity in the hippocampus. Neuron *57*, 303-313.

27. Okada, S., Igata, H., Sasaki, T., and Ikegaya, Y. (2017). Spatial representation of hippocampal place cells in a T-Maze with an aversive stimulation. Front Neur Circ *11*, 101.

28. Mamad, O., Agayby, B., Stumpp, L., Reilly, R.B., and Tsanov, M. (2019). Extrafield activity shifts the place field center of mass to encode aversive experience. eNeuro *6*.

29. Breese, C.R., Hampson, R.E., and Deadwyler, S.A. (1989). Hippocampal place cells: stereotypy and plasticity. J Neurosci *9*, 1097-1111.

30. Bostock, E., Muller, R.U., and Kubie, J.L. (1991). Experience-dependent modifications of hippocampal place cell firing. Hippocampus *1*, 193-205.

31. Anderson, M.I., and Jeffery, K.J. (2003). Heterogeneous modulation of place cell firing by changes in context. J Neurosci *23*, 8827-8835.

32. Gauthier, J.L., and Tank, D.W. (2018). A dedicated population for reward coding in the hippocampus. Neuron *99*, 179-193.e177.

33. Grill, H.J., and Norgren, R. (1978). The taste reactivity test. I. Mimetic responses to gustatory stimuli in neurologically normal rats. Brain Res *143*, 263-279.

34. Travers, J.B., and Norgren, R. (1986). Electromyographic analysis of the ingestion and rejection of sapid stimuli in the rat. Behav Neurosci *100*, 544-555.

35. Katz, D.B., Simon, S.A., and Nicolelis, M.A. (2001). Dynamic and multimodal responses of gustatory cortical neurons in awake rats. J Neurosci *21*, 4478-4489.

36. Tang, W., Shin, J.D., Frank, L.M., and Jadhav, S.P. (2017). Hippocampal-prefrontal reactivation during learning is stronger in awake compared with sleep states. J Neurosci *37*, 11789-11805.

37. Jadhav, S.P., Rothschild, G., Roumis, D.K., and Frank, L.M. (2016). Coordinated excitation and inhibition of prefrontal ensembles during awake hippocampal sharp-wave ripple events. Neuron *90*, 113-127.

38. Fontanini, A., Grossman, S.E., Figueroa, J.A., and Katz, D.B. (2009). Distinct subtypes of basolateral amygdala taste neurons reflect palatability and reward. J Neurosci *29*, 2486-2495.

39. Li, J.X., Yoshida, T., Monk, K.J., and Katz, D.B. (2013). Lateral hypothalamus contains two types of palatability-related taste responses with distinct dynamics. J Neurosci *33*, 9462-9473.

40. Piette, C.E., Baez-Santiago, M.A., Reid, E.E., Katz, D.B., and Moran, A. (2012). Inactivation of basolateral amygdala specifically eliminates palatability-related information in cortical sensory responses. J Neurosci *32*, 9981-9991.

41. Sadacca, B.F., Rothwax, J.T., and Katz, D.B. (2012). Sodium concentration coding gives way to evaluative coding in cortex and amygdala. J Neurosci *32*, 9999-10011.

42. Maier, J.X., Blankenship, M.L., Li, J.X., and Katz, D.B. (2015). A multisensory network for olfactory processing. Curr Biol *25*, 2642-2650.

43. Brun, V.H., Otnass, M.K., Molden, S., Steffenach, H.A., Witter, M.P., Moser, M.B., and Moser, E.I. (2002). Place cells and place recognition maintained by direct entorhinal-hippocampal circuitry. Science *296*, 2243-2246.

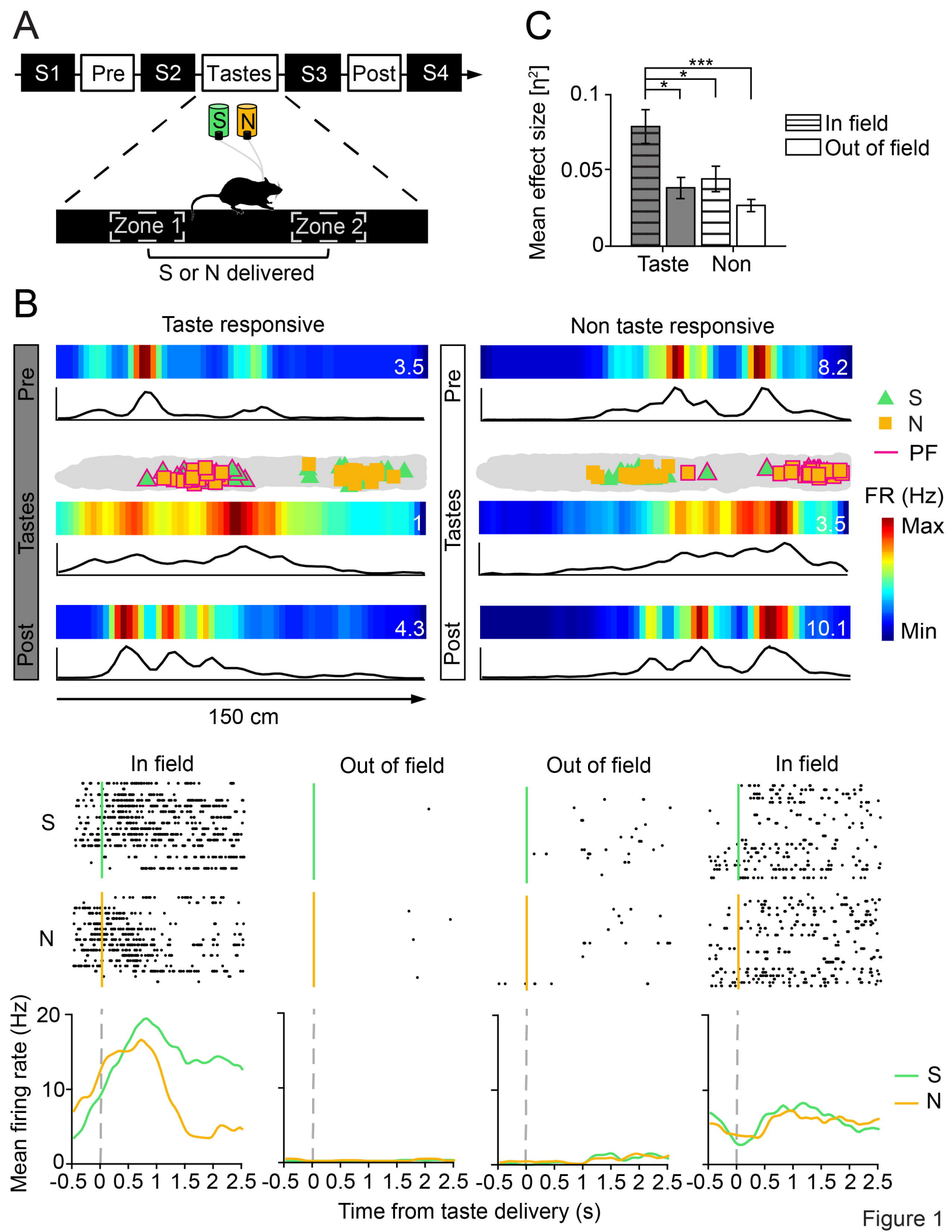
A
S1
Pre
S2
Tastes
S3
Post
S4
S
N
Zone 1
Zone 2
S or N delivered
C
Mean effect size [n²]
0.1
0.05
0
***
*
*
In field
Out of field
Taste
Non
B
Taste responsive
Non taste responsive
Pre
Tastes
Post
3.5
1
4.3
8.2
3.5
10.1
S
N
PF
FR (Hz)
Max
Min
150 cm
In field
Out of field
Out of field
In field
S
N
Mean firing rate (Hz)
20
10
0
-0.5 0 0.5 1 1.5 2 2.5
Time from taste delivery (s)

Figure 1

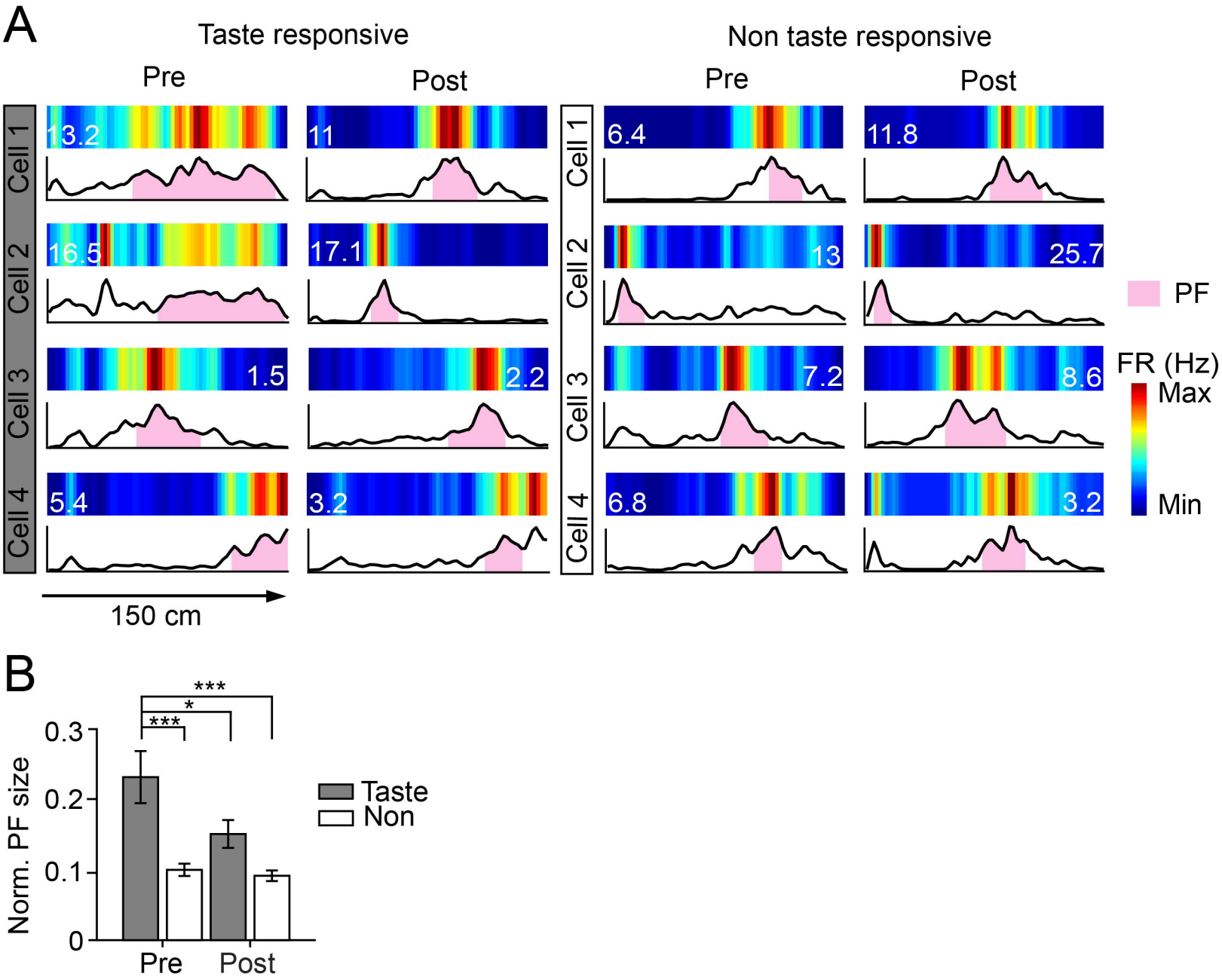
A
Taste responsive
Non taste responsive
Pre
Post
Pre
Post
Cell 1
Cell 2
Cell 3
Cell 4
13.2
11
16.5
17.1
1.5
2.2
5.4
3.2
6.4
11.8
13
25.7
7.2
8.6
6.8
3.2
PF
FR (Hz)
Max
Min
150 cm
B
Norm. PF size
0.3
0.2
0.1
0
***
*
***
Taste
Non
Pre
Post

Figure 2

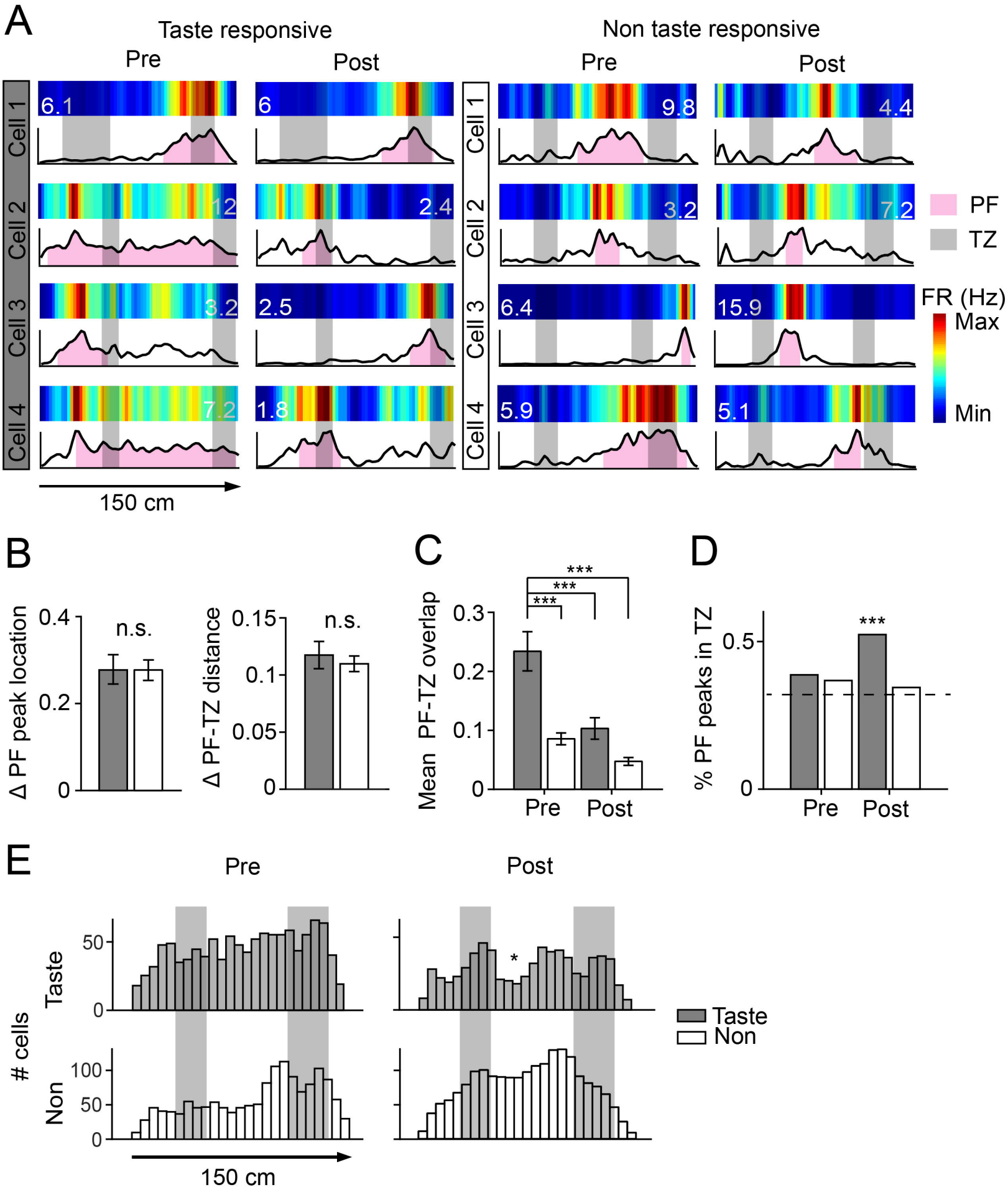
A
Taste responsive
Non taste responsive
Pre
Post
Pre
Post
Cell 1
Cell 2
Cell 3
Cell 4
6.1
6
9.8
4.4
12
2.4
3.2
7.2
3.2
2.5
6.4
15.9
7.2
1.8
5.9
5.1
PF
TZ
FR (Hz)
Max
Min
150 cm
B
Δ PF peak location
n.s.
Δ PF-TZ distance
n.s.
C
Mean PF-TZ overlap
***
***
***
Pre
Post
D
% PF peaks in TZ
***
Pre
Post
E
Pre
Post
Taste
Non
cells
*
Taste
Non
150 cm

Figure 3

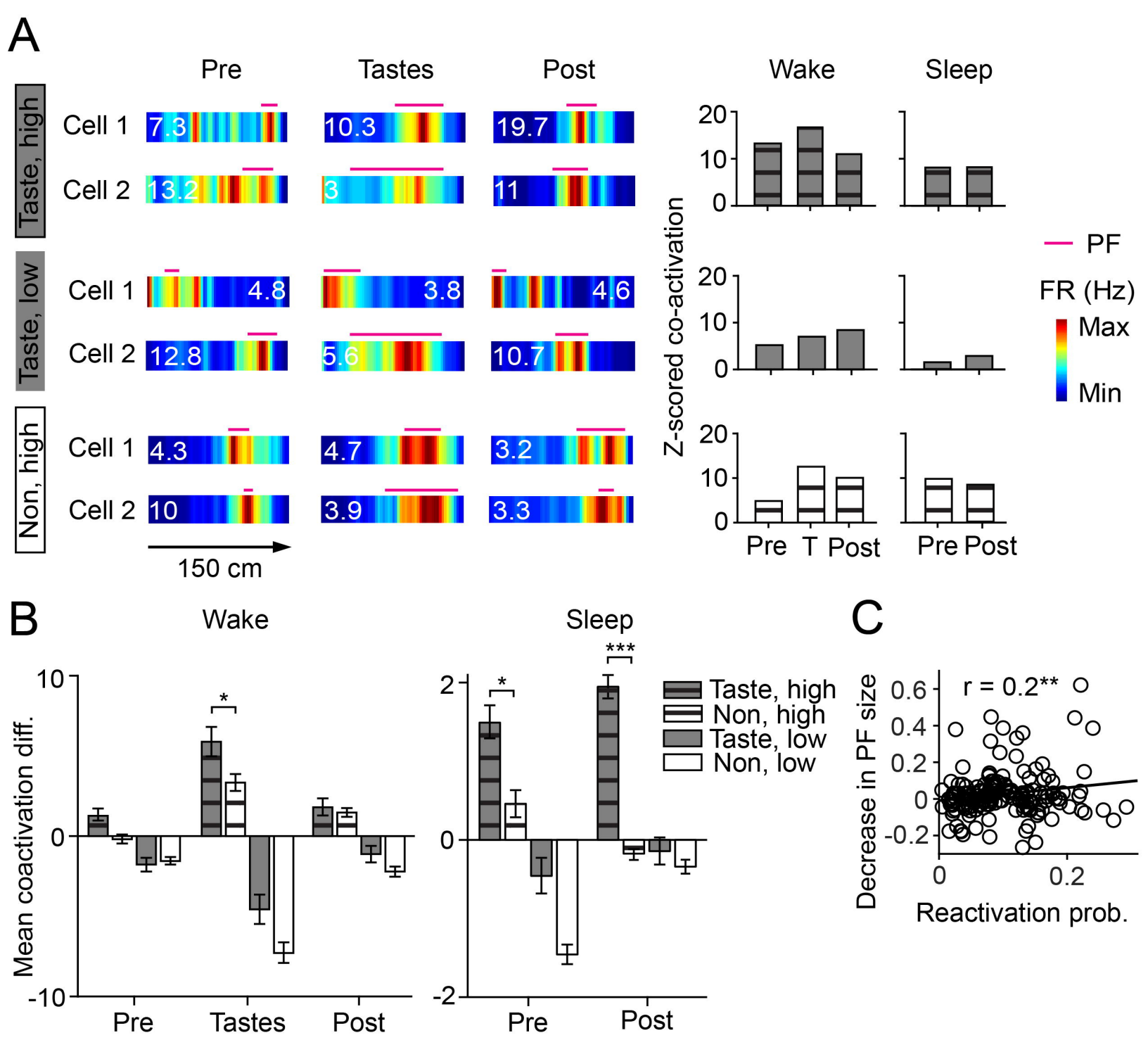
A
Pre
Tastes
Post
Wake
Sleep
Taste, high
Cell 1
Cell 2
7.3
10.3
19.7
13.2
3
11
Taste, low
4.8
3.8
4.6
12.8
5.6
10.7
Non, high
4.3
4.7
3.2
10
3.9
3.3
150 cm
Z-scored co-activation
PF
FR (Hz)
Max
Min
Pre
T
Post
B
Mean coactivation diff.
Taste, high
Non, high
Taste, low
Non, low
C
r = 0.2**
Decrease in PF size
Reactivation prob.

Figure 4